Applied and Computational Mathematics
2017; 6(3): 143-160
http://www.sciencepublishinggroup.com/j/acm
doi: 10.11648/j.acm.20170603.13
ISSN: 2328-5605 (Print); ISSN: 2328-5613 (Online)

Mathematical Analysis of Diffusion and Kinetics of Immobilized Enzyme Systems that Follow the Michaelis – Menten Mechanism

Krishnan Lakshmi Narayanan[1], Velmurugan Meena[2, *], Lakshman Rajendran[1], Jianqiang Gao[3], Subbiah Parathasarathy Subbiah[4]

[1]Department of Mathematics, Sethu Inistitute of Technology, Kariapatti, India

[2]Department of Mathematics, Madurai Kamaraj University Constitutional College, Madurai, India

[3]Department of Computer Information, Hohai University, Nanjing, China

[4]Mannar Thirumalai Naiker College, Pasumalai, Madurai, India

Email address:

lkrithick@gmail.com (K. L. Narayanan), meenakvishwa@gmail.com (V. Meena), raj_sms@rediffmail.com (L. Rajendran), jianqianggaohh@126.com (Jianqiang Gao), jasminemtnc@gmail.com (S. P. Subbiah)

[*]Corresponding author

To cite this article:

Krishnan Lakshmi Narayanan, Velmurugan Meena, Lakshman Rajendran, Jianqiang Gao, Subbiah Parathasarathy Subbiah. Mathematical Analysis of Diffusion and Kinetics of Immobilized Enzyme Systems that Follow the Michaelis – Menten Mechanism. *Applied and Computational Mathematics*. Vol. 6, No. 3, 2017, pp. 143-160. doi: 10.11648/j.acm.20170603.13

Received: April 5, 2017; **Accepted**: April 18, 2017; **Published**: June 21, 2017

Abstract: In this paper, mathematical models of immobilized enzyme system that follow the Michaelis-Menten mechanism for both reversible and irreversible reactions are discussed. This model is based on the diffusion equations containing the non-linear term related to Michaelis-Menten kinetics. An approximate analytical technique employing the modified Adomian decomposition method is used to solve the non-linear reaction diffusion equation in immobilized enzyme system. The concentration profile of the substrate is derived in terms of all parameters. A simple expression of the substrate concentration is obtained as a function of the Thiele modulus and the Michaelis constant. The numerical solutions are compared with our analytical solutions for slab, cylinder and spherical pellet shapes. Satisfactory agreement for all values of the Thiele modulus and the Michaelis constant is noted. Graphical results and tabulated data are presented and discussed quantitatively to illustrate the solution.

Keywords: Mathematical Modeling, Nonlinear Differential Equations, Modified Adomian Decomposition Method, Michaelis-Menten Kinetics, Immobilized Enzyme

1. Introduction

Many problems in theoretical and experimental biology involve reaction diffusion equations with nonlinear chemical kinetics. Such problems arise in the formulation of substrate and product material balances for enzymes immobilized within particles [1] in the description of substrate transport into microbial cells [2], in membrane transport, in the transfer of oxygen to respiring tissue and in the analysis of some artificial kidney systems [3]. For such cases, the problem is often well poised as a two-point nonlinear boundary-value problem because of the saturation, Michaelis-Menten, or Monod expressions which are used to describe the consumption of the substrate.

Mireshghi et al [4] provide a new approach for estimation of mass transfer parameters in immobilized enzymes systems. Benaiges et. al [5] studied the isomerzation of glucose into fructose using a commercial immobilized glucose-isomerase. The Michaelis-Menten equation is the most common rate expression used for enzyme reactions. This equation can also be used for immobilized enzymes [6, 7]. Many authors discussed the application of immobilized enzyme reactors extensively, but immobilized enzyme engineering is still in its infancy. Several general categories

of immobilized enzyme reactors such on: batch reactors, continuous stirred reactors, fixed bed reactors and fluidized bed reactors exist. When the immobilized enzyme is in the form of spheres, chips, discs, sheets or pellets it can be packed readily into a column [8-10].

Many authors presented enzymatic kinetics of irreversible [11-15] and reversible [14-16] mechanism. Farhad et al. [15] solved the nonlinear differential equations in enzyme kinetic mechanism using finite difference method. To the best of our knowledge, till date, no rigorous analytical expressions for the steady-state concentration for immobilized mechanisms are derived. We have presented the analytical expressions for substrate concentrations for all the three cases of kinetic models and for all possible values of the parameters using modified Adomian decomposition method [16-21]. These results are compared with the numerical results and are found to be good in the agreement. A simple analytical expression of the concentration is obtained for various particle shapes and for external mass transfer resistance boundary condition. Also, the general expressions for the mean integrated effectiveness factor for all values of parameters are presented.

2. Formulation of the Problem and Analysis

The immobilized enzyme systems may be considered to be porous slab, cylinder and sphere shapes where enzymes are uniformly distributed on the surface and in the interior. Pictorial representation of the enzyme in the biocatalyst is provided in Figure. 1.

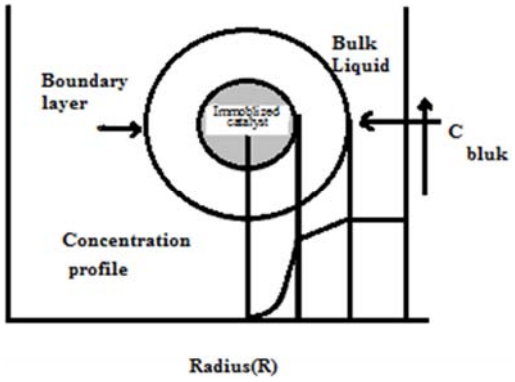

Figure 1. *Pictorial representation of the enzyme in the biocatalyst.*

It is further assumed that: (1) The kinetics of the free enzyme are described by the Michaelis-Menten equation for irreversible reactions and by the modified Michaelis-Menten equation for reversible reactions; (2) No partition effect exists between the particle surface and the interior; (3) The temperature, density, and effective diffusivity of reactants inside the particle are constant; (4) A quasi-steady-state condition is attained; (5). The partition effect between the support and bulk fluid phase is neglected; (6) Enzyme deactivation is neglected. Based on these above assumptions, the governing differential equations with boundary conditions for irreversible and reversible reactions are reported below.

Nomenclature

Symbols	Définitions	Units
a	Volume of the fluid phase in the reactor	none
Bi	Biot number reaction in the pellet	none
C	Dimensionless substrate concentration for the reversible reaction in the pellet	none
$\bar{C}$	Dimensionless substrate concentration for the reversible reaction in the pellet	none
D_e	Effective diffusivity of the substrate in the pellet	cm^2 / min
Ef	Effective factor	none
g	Pellet shape factor	none
k_1	External mass-transfer co-efficient	cm/s
K_m	Irreversible reaction Michaelis constant	kg/m^3
$K_m^{'}$	Reversible reaction Michaelis constant	kg/m^3
K_{mf}	Reversible reaction Michaelis constant	M
K_{mr}	Michaelis constant of the reverse reaction	M
v_0	Initial reaction rates	none
V_m	Irreversible maximum reaction rate	$kg/s/m^3$ cat
V_{mf}	Reversible maximum reaction rate	$kg/s/m^3$ cat
V_{mr}	Maximum velocity of the reverse reaction	mol / min/ l cat
R	Half-thickness of the pellet	m
S	Irreversible substrate concentration inside the pellet	$\mu\ mol/cm^3$
S_{eq}	Equilibrium substrate concentration	$\mu\ mol/cm^3$
$\bar{S}$	Reversible substrate concentration inside the pellet	$\mu\ mol/cm^3$
S_b	Irreversible substrate concentration in the bulk fluid phase	$\mu\ mol/cm^3$
S_{b0}	Irreversible initial substrate concentration in the bulk fluid phase	$\mu\ mol/cm^3$
$\bar{S}_b$	Reversible substrate concentration in the bulk fluid phase	$\mu\ mol/cm^3$
$\bar{S}_{b_0}$	Reversible substrate concentration in the bulk fluid phase	$\mu\ mol/cm^3$
t	Time	min
X	Dimensionless distance	none
x	Distance to the center	none
Y	Dimensionless reversible substrate concentration	none
Greek symbols		
α	Dimensionless parameter in reversible reaction	none

β_b	Dimensionless parameter in irreversible reaction for bulk fluid phase	none
$\bar{\beta}_b$	Dimensionless parameter in reversible reaction for bulk fluid phase	none
β_{b0}	Dimensionless parameter for initial fluid phase	none
ϕ	Intrinsic modified Thiele modulus in irreversible reaction	none
$\bar{\phi}$	Dimensionless parameter in irreversible reaction	none

2.1. Irreversible Reactions

A differential mass balance equation for the substrate for irreversible reactions in dimensionless form can be represented as follows [15]:

$$\frac{d^2C}{dX^2}+\frac{g-1}{X}\frac{dC}{dX}=\phi^2\frac{C}{1+\beta_b C} \tag{1}$$

The boundary conditions are given by

$$X=0,\frac{dC}{dX}=0 \tag{2}$$

$$\mathrm{X}=1,\ \mathrm{C}=1 \text{ (without external mass transfer resistance)} \tag{3}$$

$$X=1,\frac{dC}{dX}=Bi(1-C) \text{ (with external mass transfer resistance)} \tag{4}$$

where C represents the dimensionless substrate concentration, X represents the dimensionless distance to the center or the surface of symmetry of the pellet, ϕ, β_b and Bi represents the Thiele module, dimensionless parameter for bulk fluid phase and Biot number respectively. The g characterizes the shape of the immobilized catalyst with g =1, 2, 3 for a slab, cylindrical, and spherical pellets respectively. So it can be regarded as a 'shape factor' for the particle. The dimensionless variables are defined as follows:

$$C=\frac{S}{S_b},\ X=\frac{x}{R},\ \beta_b=\frac{S_b}{K_m},\ \phi=R\sqrt{\frac{V_m}{K_m D_e}} \text{ (Theile modulus)},\ Bi=R\frac{K_1}{D_e} \text{ (Biot number)} \tag{5}$$

In the above expressions, the parameters x, R, K_1, D_e, S and S_b represent the distance to the center, the half-thickness of the pellet, the external mass transfer coefficient, the effective diffusivity of the substrate in the pellet, the substrate concentration inside the pellet and substrate concentration in the bulk fluid phase respectively. K_m and V_m are the kinetic parameters. The equation (1) also describes the temperature or concentration variation in many fields of physics, chemistry, biology, biochemistry, and many others [7–14]. The effectiveness factor, Ef is given by

$$Ef = g\left(1+\beta_b\right)\int_0^1 \frac{C}{\left(1+\beta_b C\right)}X^{g-1}dX \tag{6}$$

The initial substrate reaction rate v_0 is given by

$$v_0 = Ef\ \frac{V_m S_{b0}}{K_m + S_{b0}} \tag{7}$$

where S_{b0} denotes the initial substrate concentration.

2.2. Reversible Reactions

For reversible reactions, the governing differential equation for the dimensionless substrate concentration in the pellets is the same as Eq. 1 except the following dimensionless parameters.

$$\bar{C}=\frac{\bar{S}}{\bar{S}_b},\ \bar{\beta}_b=\frac{\bar{S}_b}{K_m'},\ \bar{\phi}=R\sqrt{\frac{V_m'}{K_m' D_e}},\ \bar{S}_b=S-S_{eq} \tag{8}$$

where $\bar{C}$, $\bar{\phi}$, $\bar{\beta_b}$ and $\bar{S_b}$ represents dimensionless substrate concentration, the Thiele module, dimensionless parameter for bulk fluid phase and substrate concentration in the bulk fluid phase for reversible reaction. $\bar{S}$ represents the substrate concentration inside the pellet, S_{eq} is the equilibrium substrate concentration, $V_m^{'}$ represents the maximum reaction rate and $K_m^{'}$ is the Michaelis constants. The rate of change of substrate concentration Y in batch reactor can be written as

$$\frac{dY}{dt}=\alpha\frac{Y}{1+\beta_{b0}Y} \tag{9}$$

where

$$Y=\frac{\bar{S}_b}{\bar{S}_{b0}},\ \alpha=\frac{-a\,E\bar{f}\,V_m'}{K_m'},\ \beta_{b0}=\frac{\bar{S}_{b0}}{K_m'},\ \bar{S}_{b0}=S_{b0}-S_{eq} \tag{10}$$

where α represent the ratio of the catalyst volume to the volume of the fluid phase reactor, a (= 0.0252) is the ratio of the catalyst volume to the volume of fluid phase in the reactor. The Eqn. (9) is solved with the initial condition $Y(t=0)=1$.

3. Analytical Expression of the Concentration for Irreversible and Reversible Reactions Using MADM

In the recent years, much attention is devoted to the application of the modified Adomian decomposition method (MADM) to the solution of various non-linear problems in physical and chemical sciences. This method is used to find the approximate analytical solution in terms of a rapidly

convergent infinite power series with easily computable terms [17-18]. In other words, the zeroth component used in the standard ADM can be divided into the two functions [19-21]. The ADM is unique in its applicability, accuracy and efficiency and only a few iterations are needed to find the asymptotic solution. The basic concept of the method is given in Appendix A.

3.1. Irreversible Reaction Without External Mass Transfer Resistance

Solving equation (1) using this method (see Appendix B), we obtain the concentration of the immobilized catalyst with g =1, 2, 3 for a slab, cylindrical, and spherical pellets as follows:

$$C(X)=1+\frac{1}{2g}\left[\frac{\phi^2}{(1+\beta_b)}\left(X^2-1\right)+\frac{\phi^4}{60\,(1+\beta_b)^3}\left(3X^4-10\,X^2+7\right)\right] \quad (11)$$

Effective factor Ef for slab, cylindrical and spherical is

$$Ef=1-\frac{\phi^2}{15\left(1+\beta_b\right)^2} \quad (12)$$

Using Eqns. (7) and (12) the initial substrate reaction rate v_0 can be obtained as follows:

$$v_0=\left(1-\frac{\phi^2}{15\left(1+\beta_b\right)^2}\right)\frac{V_m\,S_{b0}}{K_m+S_{b0}} \quad (13)$$

3.2. Irreversible Reaction with External Mass Transfer Resistance

The substrate concentration with external mass transfer resistance for the initial and boundary conditions (Eqns. (2) and (4)) is obtained (see Appendix C) from Eqn. (1) as follows:

$$C(X)=1+\frac{1}{2g}\left\{\frac{\phi^2}{(1+\beta_b)}\left[X^2-\frac{2}{Bi}-1\right]+\frac{\phi^4}{\left(1+\beta_b\right)^3}\left[\frac{1}{20}(X^4-1)-\frac{1}{3}\left(\frac{1}{Bi}+\frac{1}{2}\right)\left(X^2-\frac{2}{Bi}-1\right)-\frac{1}{5Bi}\right]\right\} \quad (14)$$

The change in reaction rate can be expressed quantitatively by introducing the effectiveness factor, Ef. Using Eqn. (6), effective factor for slab, cylindrical and spherical is

$$Ef=1-\frac{2\phi^2}{5\left(1+\beta_b\right)^2} \quad (15)$$

Using Eqns. (7) and (15), the initial substrate reaction rate v_0 can be obtained as follows:

$$v_0=\left(1-\frac{2\phi^2}{5\left(1+\beta_b\right)^2}\right)\frac{V_m\,S_{b0}}{K_m+S_{b0}} \quad (16)$$

Summary of all the expression of substrate concentration and effectiveness factor for with and without external mass transfer resistance are also given in Table 1.

Table 1. *Substrate concentration and effective factor in the with and without external mass transfer resistance.*

Resistance	Substrate concentration	Fig.	Effectiveness factors	Fig.	Initial Reaction rate
Without external mass transfer resistance	$C(X)=1+\frac{1}{2g}\left(\frac{\phi^2}{(1+\beta_b)}\left(X^2-1\right)+\frac{\phi^4}{60\,(1+\beta_b)^3}\left(3X^4-10\,X^2+7\right)\right)$ Eq. (11)	Fig. 1-3 8, 10(a)	$Ef=1-\frac{\phi^2}{15\left(1+\beta_b\right)^2}$ Eq. (12)	Fig. 9(a)	$v_0=\left(1-\frac{\phi^2}{15\left(1+\beta_b\right)^2}\right)\frac{V_m\,S_{b0}}{K_m+S_{b0}}$ Eq. (13)
With external mass transfer resistance	$C(X)=1+\frac{1}{2g}\left(\frac{\phi^2}{(1+\beta_b)}\left[X^2-\frac{2}{Bi}-1\right]+\frac{\phi^4}{(1+\beta_b)^3}\left[\frac{1}{20}(X^4-1)-\frac{1}{3}\left[\frac{1}{Bi}+\frac{1}{2}\right]\right]\left[X^2-\frac{2}{Bi}-1\right]-\frac{1}{5Bi}\right]\right)$ Eq. (14)	Fig. 4-6 9, 10(b)	$Ef=1-\frac{2\phi^2}{5\left(1+\beta_b\right)^2}$ Eq. (15)	Fig. 9(b)	$v_0=\left(1-\frac{2\phi^2}{5\left(1+\beta_b\right)^2}\right)\frac{V_m\,S_{b0}}{K_m+S_{b0}}$ Eq. (16)

3.3. Reversible Reaction

By replacing the variables C, ϕ and β_b by $\overline{C}$, $\overline{\phi}$, $\overline{\beta}_b$ in the Eqns. (11 -14), we can obtain the concentration of substrate and effective factor of reversible reaction.

4. Analytical Expression of the Concentration of Substrate Using the New Approach of HPM

The advantage of the new homotopy perturbation method (HPM) is that it does not need a small parameter in the

system [32]. Recently, many authors have used HPM for various problems and reported the efficiency of the HPM to handling nonlinear engineering problems [33-35]. Recently, a new approach to HPM is introduced to solve the nonlinear problem, in which one will get better simple approximate solution in the zeroth iteration [19]. In this paper, a new approach to the Homotopy perturbation method is applied (Appendix D) to solve the nonlinear differential equation (9). Using this method, the analytical expressions of the substrate concentrations can be obtained as follows:

$$Y(t) = \frac{\overline{S}_b}{\overline{S}_{b0}} = \exp\left(-\frac{\alpha}{1+\beta_{b0}}t\right) = \exp\left(\frac{-a\,\overline{Ef}\;V_m^{'}}{\overline{S}_{b0}}t\right) \qquad (17)$$

5. Numerical Simulation

The non-linear differential equations (1) and (7) for the given initial boundary conditions are solved numerically using the Matlab program [36]. The numerical values of parameters used in this work are given in Table 2 and Table 3. Its numerical solution is compared with our analytical results in Tables (3) – (5) and it gives satisfactory agreement. In all the case, the average relative error is less than 1.3%. The Matlab program is also given in Appendix-E and F.

Table 2. *Summarized description of the immobilized enzyme systems investigated [24].*

Case no.	1	2	3	4
Enzyme	Amyloglucocidase	Amyloglucocidase	Gulcoseisomerase	Sweetzyme Q
Support	Honey ceramic slab	Porous spherical Glass beads	Porous spherical Glass beads	spherical beads
reaction	irreversible	Irreversible	reversible	reversible
substrate	Soluble starch	Dextrin	Glucose	Glucose
Product	Glucose	Glucose	Fructose	Fructose
Reactor	Stirred batch reactor	Recycling differential batch reactor	Recycling differential batch reactor	Stirred batch reactor
$D_e\,(cm^2/s)$	3.67 x 10^{-8}	5.30 x 10^{-7}	1.36 x 10^{-6}	8.33 x 10^{-7}
$k_1\,(cm/s)$	negligible	Negligible	9.52 x 10^{-3}	negligible
R (m)	1.6 x 10^{-4}	1.6 x 10^{-4}	1.6 x 10^{-4}	3.2 x 10^{-5}
$K_m\;\;(kg/m^3)$	0.258	0.25042	-	-
$V_m\;\;(kg/s/m^3 cat)$	2.51 x 10^{-2}	0.4429	-	-
$K_{mf}(M)$	-	-	0.211	0.452
$V_{mf}\,(mol/\min/lcat)$	-	-	0.1453 x10^{-3}	0.142
$K_{mr}(M)$	-	-	0.389	-
$V_{mr}\,(mol/\min/lcat)$	-	-	2.783 x10^{-3}	-
Figure	10	See in the subblimendary material	See in the subblimendary material	See in the subblimendary material
References	[39]	[18]	[40]	[8]

Table 3. *Numerical values of the parameter using this work.*

Parameter	Case 1	Case 2	Case 3		Case 4
Thiele Module	$\phi = R\sqrt{V_m/(K_m D_e)}$		Forward $\phi = R\sqrt{V_m/(K_m D_e)}$	Backward $\phi = R\sqrt{V_m/(K_m D_e)}$	Forward $\phi = R\sqrt{V_m/(K_m D_e)}$
	0.2605	2.1092	0.0035	0.0035	0.0197
Dimensionless parameter in reaction for bulk fluid phase	$\beta_b = S_b/K_m$		$\overline{\beta_b} = \overline{S_b}/K_{mf}^{'}$	$\overline{\beta_b} = \overline{S_b}/K_{mr}^{'}$	$\overline{\beta_b} = \overline{S_b}/K_{mf}^{'}$
	337.054	56.65	412.132	223.54	192.38
Effectiveness factor $Ef = 1 - \frac{\phi^2}{15(1+\beta_b)^2}$	0.99	0.99	1	0.99	0.99

Table 4. *Comparison of dimensionless substrate concentration* C *(without mass transfer resistance) with numerical result for various values of* ϕ and β_b.

(a) Spherical particle

g	X	$\phi = 5$				$\phi = 10$			
		β_b	Our Work Eqn. (11)	Numerical	% Error	β_b	Our Work Eqn. (11)	Numerical	% Error
3	0.0	2	0.161	0.163	1.22	15	0.105	0.107	1.86
	0.2	5	0.406	0.413	1.69	20	0.277	0.282	1.77
	0.4	7	0.581	0.581	0	25	0.470	0.470	0
	0.6	10	0.762	0.762	0	50	0.791	0.791	0
	0.8	15	0.907	0.907	0	100	0.940	0.940	0
	1.0	10	1.000	1.000	0	500	1.000	1.000	0
		Average deviation			0.582	Average deviation			0.728

g	X	$\beta_b = 1$				$\beta_b = 5$			
		ϕ	Our Work Eqn. (11)	Numerical	% Error	ϕ	Our Work Eqn. (11)	Numerical	% Error
3	0.0	4	0.282	0.288	2.08	6	0.211	0.215	1.86
	0.2	3	0.463	0.465	0.43	5	0.413	0.416	0.72
	0.4	2.5	0.636	0.636	0	4	0.644	0.644	0
	0.6	2	0.807	0.807	0	3	0.843	0.843	0
	0.8	1.5	0.935	0.935	0	2	0.960	0.960	0
	1.0	0.1	1.000	1.000	0	1	1.000	1.000	0
		Average deviation			0.502	Average deviation			0.516

(b) cylinder particle

g	X	$\phi = 2$				$\phi = 10$			
		β_b	Our Work Eqn. (11)	Numerical	% Error	β_b	Our Work Eqn. (11)	Numerical	% Error
2	0.0	0.1	0.440	0.455	2.220	25	0.055	0.130	2.31
	0.2	1	0.575	0.598	3.380	35	0.349	0.353	1.69
	0.4	2	0.733	0.744	1.350	50	0.589	0.592	0
	0.6	5	0.894	0.895	0	75	0.790	0.790	0
	0.8	10	0.967	0.967	0	100	0.910	0.911	0
	1.0	50	1.000	1.000	0	300	1.000	1.000	0
		Average deviation			1.38	Average deviation			0.8

g	X	$\beta_b = 1$				$\beta_b = 5$			
		ϕ	Our Work Eqn. (11)	Numerical	% Error	ϕ	Our Work Eqn. (11)	Numerical	% Error
2	0.0	3	0.300	0.306	1.96	5	0.202	0.206	1.94
	0.2	2.5	0.454	0.458	0.87	4	0.432	0.438	1.36
	0.4	2	0.655	0.655	0	3.5	0.587	0.587	0
	0.6	1.5	0.829	0.829	0	3	0.765	0.765	0
	0.8	1	0.955	0.956	0	2	0.940	0.940	0
	1.0	0.1	1.000	1.000	0	1	1.000	1.000	0
		Average deviation			0.566	Average deviation			0.66

(c) Slab particle

g	X	$\phi = 1.5$				$\phi = 5$			
		β_b	Our Work Eqn. (11)	Numerical	% Error	β_b	Our Work Eqn. (11)	Numerical	% Error
1	0.0	1	0.554	0.564	1.773	20	0.428	0.431	0.696
	0.2	2	0.670	0.681	1.615	25	0.540	0.549	1.630
	0.4	3	0.767	0.770	0.518	30	0.662	0.662	0
	0.6	5	0.880	0.883	0	50	0.843	0.843	0
	0.8	10	0.963	0.963	0	100	0.955	0.955	0
	1.0	15	1.000	1.000	0	500	1.000	1.000	0
		Average deviation			0.78	Average deviation			0.465

g	X	$\beta_b = 1$				$\beta_b = 5$			
		ϕ	Our Work Eqn. (11)	Numerical	% Error	ϕ	Our Work Eqn. (11)	Numerical	% Error
1	0.0	1.5	0.554	0.564	1.77	3	0.271	0.373	2.70
	0.2	1.4	0.596	0.607	1.90	2.5	0.509	0.519	1.96
	0.4	1.2	0.705	0.709	0.50	2	0.723	0.735	1.36
	0.6	1	0.843	0.853	1.76	1.5	0.880	0.880	0
	0.8	0.7	0.956	0.956	0	1.2	0.956	0.956	0
	1.0	0.01	1.000	1.000	0	0.1	1.000	1.000	0
		Average deviation			1.18	Average deviation			1.20

Table 5. *Comparison of dimensionless substrate concentration C (with mass transfer resistance) with numerical results for various values of ϕ, β_b, and B_i.*

(a) Slab Particle

g	X	$\phi = 1,\ Bi = 5$				$\phi = 1,\ \beta_b = 1$			
		β_b	Our Work Eqn. (13)	Numerical	% Error	Bi	Our Work Eqn. (13)	Numerical	% Error
1	0.0	1	0.764	0.765	0.13	5	0.752	0.761	1.31
	0.2	1.5	0.754	0.755	1.43	5.5	0.809	0.813	1.23
	0.4	2.5	0.835	0.835	0	6	0.845	0.845	0
	0.6	5	0.913	0.913	0	7	0.897	0.897	0
	0.8	10	0.965	0.965	0	8	0.957	0.957	0
	1.0	15	0.987	0.987	0	15	0.993	0.993	0
Average deviation					0.312	Average deviation			0.508

(b) Cylinder Particle

g	X	$\phi = 1,\ Bi = 0.5$				$\phi = 1,\ \beta_b = 2$			
		β_b	Our Work Eqn. (13)	Numerical	% Error	Bi	Our Work Eqn. (13)	Numerical	% Error
2	0.0	2	0.637	0.6414	1.24	0.5	0.640	0.641	0.15
	0.2	3	0.704	0.715	.071	0.75	0.725	0.727	0.27
	0.4	4	0.765	0.765	0	1	0.784	0.784	0
	0.6	6	0.836	0.836	0	2	0.867	0.867	0
	0.8	10	0.901	0.901	0	5	0.937	0.937	0
	1.0	15	0.937	0.937	0	10	0.983	0.983	0
Average deviation					0.26	Average deviation			0.084

(c) Spherical Particle

g	X	$\phi = 1,\ Bi = 1$				$\phi = 1,\ \beta_b = 1$			
		β_b	Our Work Eqn. (13)	Numerical	% Error	Bi	Our Work Eqn. (13)	Numerical	% Error
3	0.0	0.1	0.661	0.664	0.45	0.5	0.650	0.658	1.21
	0.2	0.5	0.721	0.726	0.69	1	0.775	0.778	0.38
	0.4	1	0.787	0.787	0	1.5	0.832	0.832	0
	0.6	2	0.859	0.859	0	2	0.871	0.871	0
	0.8	10	0.964	0.964	0	5	0.938	0.938	0
	1.0	100	0.996	0.996	0	20	0.991	0.991	0
Average deviation					0.228	Average deviation			0.318

6. Result and Discussion

Eqns. (11-12) and (14-15) represent the analytical expression for the dimensionless substrate concentration $C(X)$ and effectiveness factor Ef for both reversible and irreversible reactions without and with mass transfer resistance for slab, cylinder and spherical pellets respectively. The substrate concentration C against the dimensionless radial distance X for the both reversible and irreversible reactions is plotted in Figs. 2 – 7 for various values of the Thiele modulus ϕ and β_b for the three shapes. When the Thiele modulus or Half – thickness of the pellet (R) increases, the substrate concentration inside catalyst will also decrease in all the cases.

Figs. 2 (a) - 4 (a) represents that the substrate concentration C versus distance X for various values of ϕ and β_b without external mass transfer resistance. The substrate concentration increases with increasing β_b or increasing irreversible substrate concentration in the bulk fluid phase (S_b) and decreasing the irreversible reaction Michaelis constant (K_m). From these figures, it is obvious that the substrate concentration reaches a uniform value when the Thiele modulus $\phi \le 0.01$ and $\beta_b > 200$. Figs. 2 (b) – 4 (b) shows that, the substrate concentration decreases with increasing the Thiele modulus ϕ or increasing Half – thickness of the pellet (R) and irreversible maximum reaction rate (V_m).

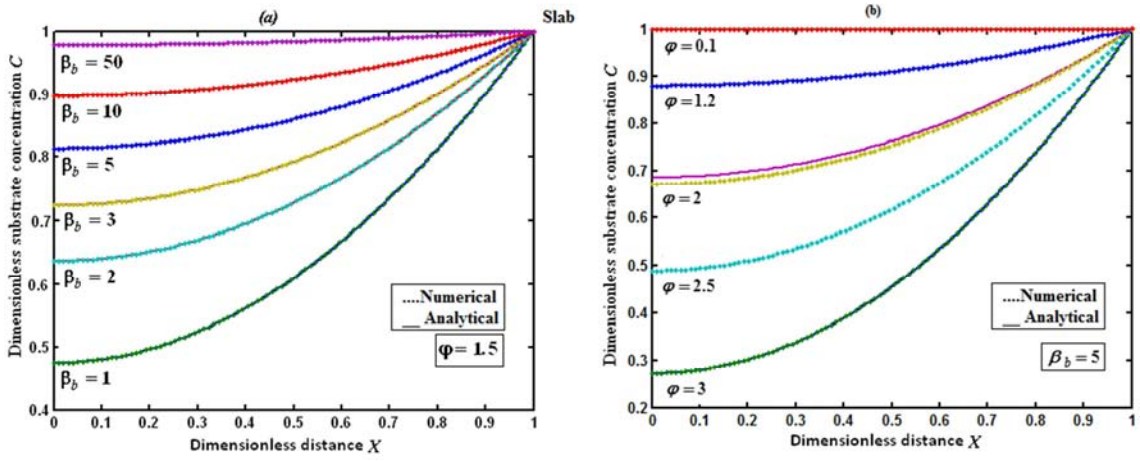

(a). $\phi = 1.5$ and $\beta_b = 1$ to 50 (b). $\beta_b = 5$ and $\phi = 0.1$ to 3

Figure 2. *Plot the dimensionless substrate concentration* C *versus dimensionless distance* X *, in the slab pellet calculated using Eqn. (11).*

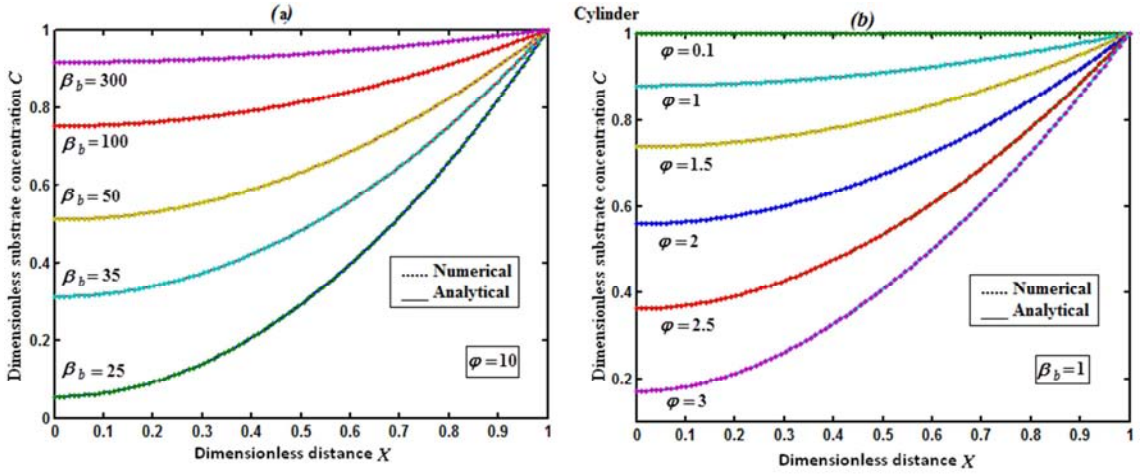

(a) $\phi = 10$ and $\beta_b = 25$ to 300 (b). $\beta_b = 1$ and $\phi = 0.1$ to 3

Figure 3. *Plot the dimensionless substrate concentration* C *versus dimensionless distance* X *, in the cylinder pellet calculated using Eqn. (11).*

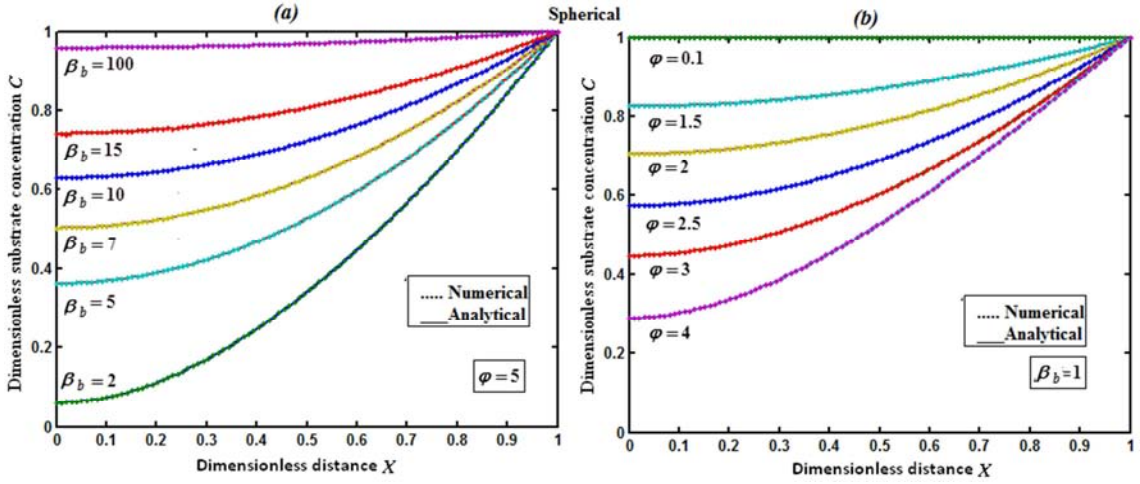

(a). $\phi = 5$ and $\beta_b = 2$ to 100 (b). $\beta_b = 1$ and $\phi = 0.1$ to 4

Figure 4. *Plot the dimensionless substrate concentration* C *versus dimensionless distance* X *, in the spherical pellet calculated using Eqn. (11).*

From Figs. (5-7) it is inferred that substrate concentration increases with the increasing Biot number (B_i) and Michaelis-Menten constant (β_b). The dimensionless substrate concentrations for the three pellets are plotted in Figs. (8). From these figures, it is concluded that the dimensionless substrate concentration for the spherical pellets is greater than slab and cylindrical pellets.

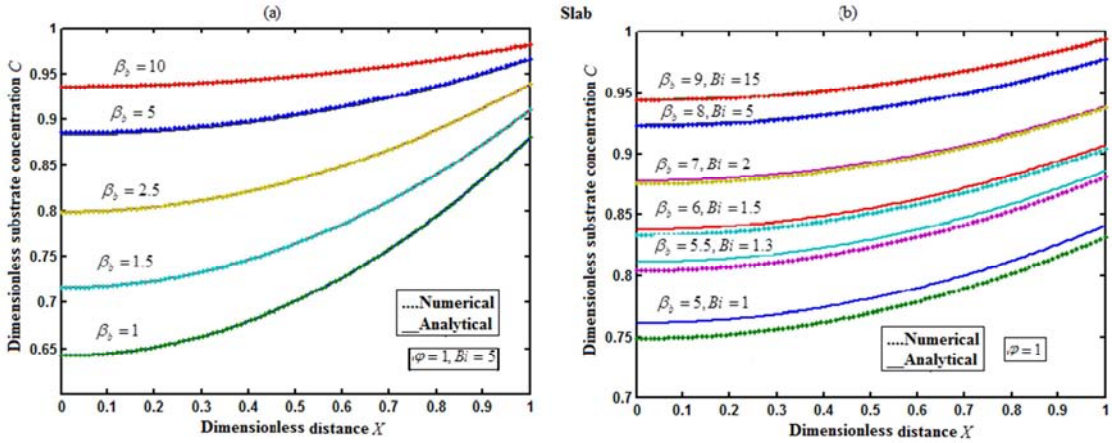

(a). $\phi = 1$, $\beta_b = 1$ and $Bi = 1$ to 15 (b). $\phi = 1, Bi = 5$ and $\beta_b = 1$ to 10

Figure 5. *Plot the dimensionless substrate concentration C versus dimensionless distance X , in the slab pellet calculated using Eqn. (14).*

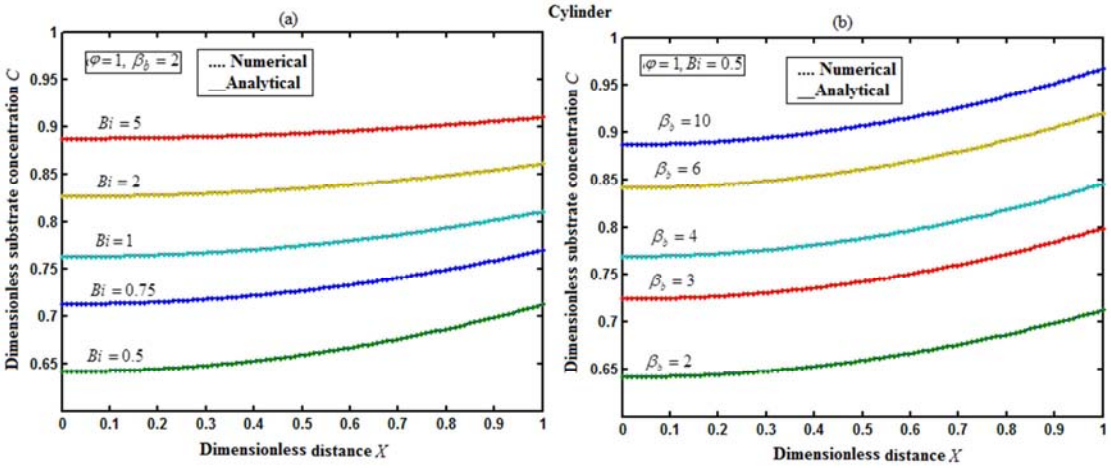

(a). $\phi = 1$, $\beta_b = 2$ and $Bi = 0.5$ to 5 (b). $\phi = 1, Bi = 0.5$ and $\beta_b = 2$ to 10

Figure 6. *Plot the dimensionless substrate concentration C versus dimensionless distance X , in the cylinder pellet calculated using Eqn. (14).*

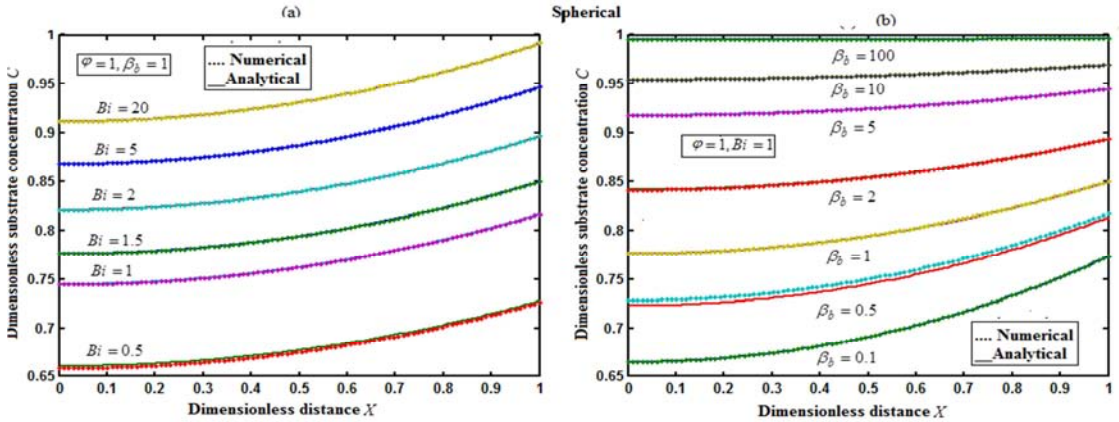

(a). $\phi = 1$, $\beta_b = 1$ and $Bi = 0.5$ to 20 (b). $\phi = 1, Bi = 1$ and $\beta_b = 0.1$ to 100 .

Figure 7. *Plot the dimensionless substrate concentration C versus dimensionless distance X , in the spherical pellet calculated using Eqn. (14).*

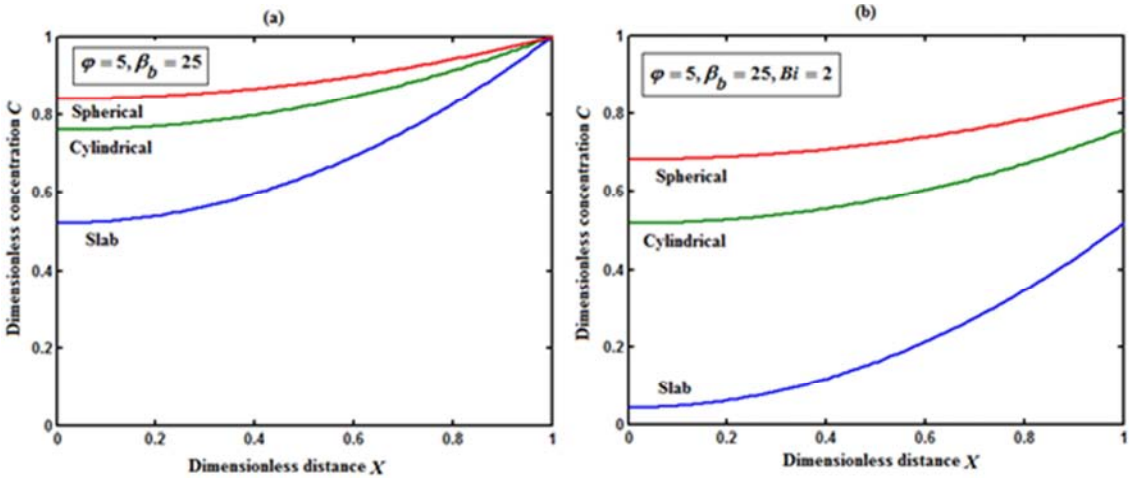

Figure 8. *Plot of dimensionless substrate concentration C versus the dimensionless distance X for the slab, cylindrical, spherical pellets (a) without mass-transfer resistance (Eqns. (11)), (b) with mass transfer resistance (Eqn. (14)).*

Plot of effectiveness factor Ef against Thiele modulus ϕ and Michaelis - Menten constant β_b is shown in Fig. 9 (*a* - b). Effectiveness factor is a dimensionless pellet production rate that measures how effectively the catalyst is being used. For η near unity, the entire volume of the pellet is reacting at the same high rate because the reactant is able to diffuse quickly through the pellet. For η near zero, the pellet reacts at low rate. The reactant is unable to penetrate significantly into the interior of the pellet and the reaction rate is small in a large portion of the pellet volume. The effectiveness factor decreases from its initial value, when the diffusional restriction or β_b increases. The effectiveness factor is maximum ($Ef \approx 1$) at lower values of ϕ and β_b . For all the cases, $Ef \approx 1$.

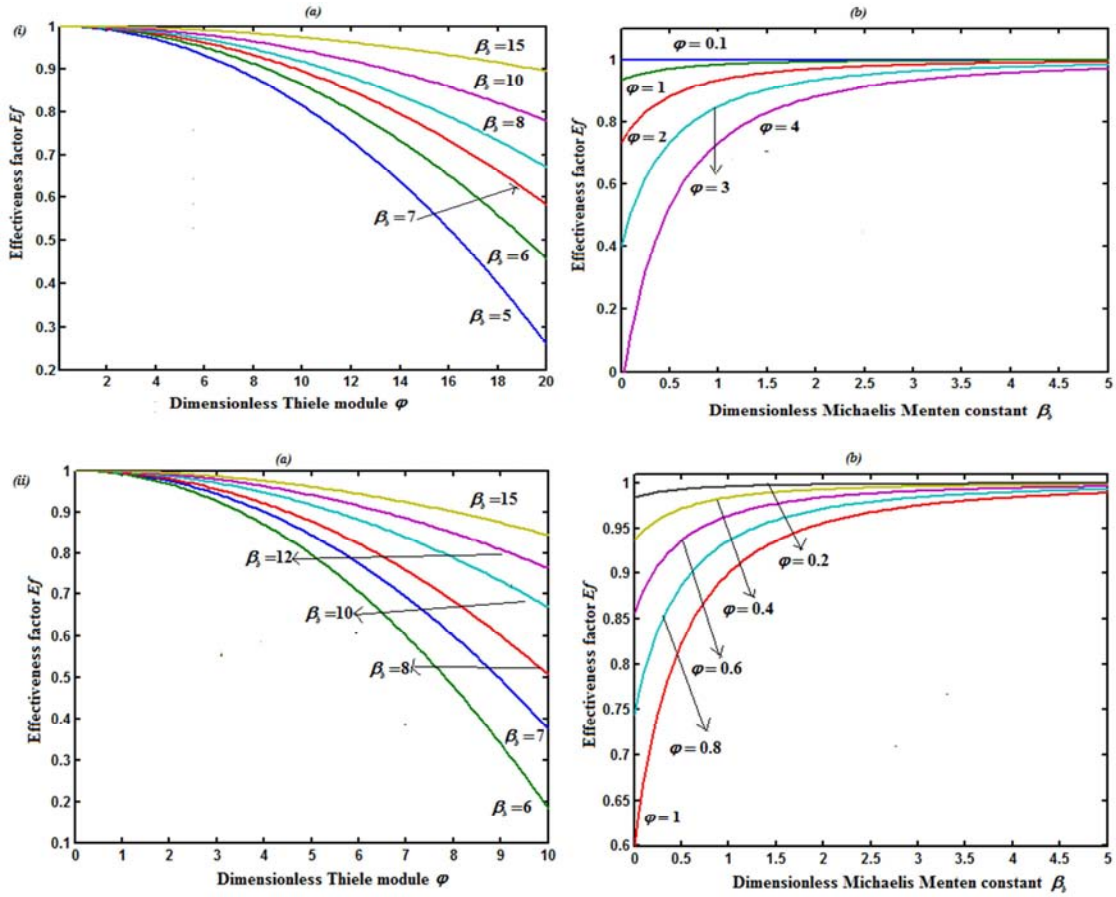

(i) (a-b) Without mass transfer resistance using (Eqn. (12)), (ii) (a-b) With mass transfer resistance using (Eqn. (15)).

Figure 9. *The general effectiveness factor Ef against Thiele modulus ϕ and Michaelis-Menten constant β_b .*

Now the Eqn. (7) can be written as follows $S_{b0}/v_0 = (K_m/V_m)+(S_{b0}/V_m)$. The plot of Fig. 10 represents S_{b0}/v_0 versus irreversible initial substrate concentration in the bulk fluid phase S_{b0} gives the slope = $1/V_m$ and the intercept= K_m/V_m. The parameters K_m and V_m are obtained from the above slope and intercept results. Good agreement between predicted and experimental data is observed at low initial substrate concentrations.

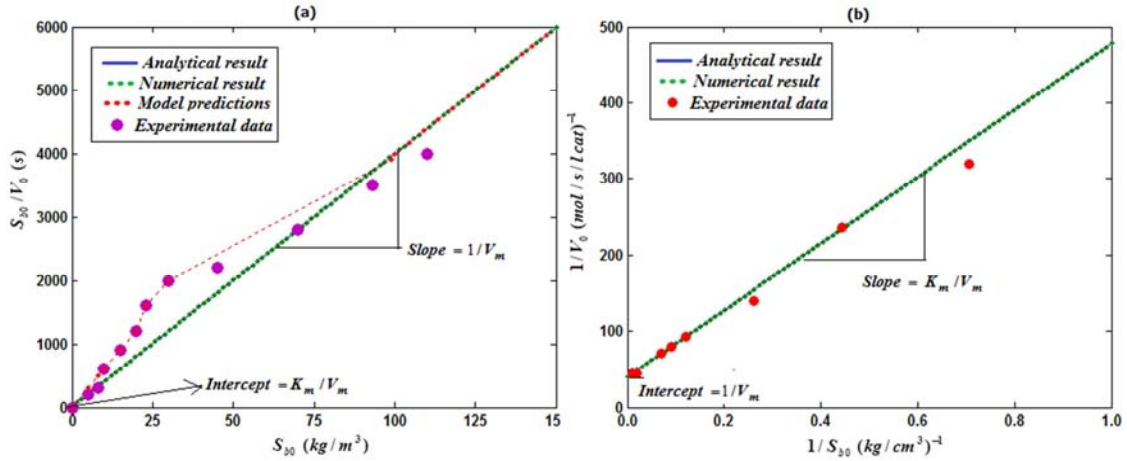

(a). Hanes-Woolf plot (b). Line weaver- Burk plot

Figure 10. *Comparison of our analytical result (Eqn. (13)) initial substrate reaction rate with the numerical result [24] and experimental data [24] (Refer Table 3) for case 1.*

Our analytical expression (Eqn. (17)) for the concentration of substrate $\overline{S}_b\,(=Y(t)\,\overline{S}_{b0})$ is compared with the experimental results in Fig. (11). Good agreement with the experimental data is noted. From this figure, it is inferred that reversible substrate concentration $\overline{S}_b$ is almost uniform when the initial bulk substrate concentration $\overline{S}_{b0}$ is constant. The substrate concentration in the fluid phase $\overline{S_b}$ increases when the initial bulk substrate concentration $\overline{S}_{b0}$ increases.

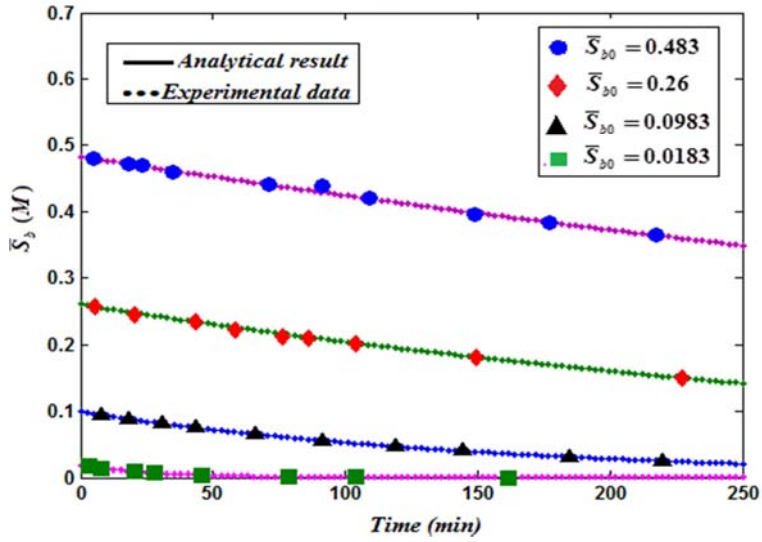

Figure 11. *Comparison of our analytical result (Eqn. (17)) for substrate concentration with the numerical result [24] and experimental data [24] for the time courses of substrate consumption in a batch reactor model (Refer Table 3).*

7. Conclusions

In this paper an approximate analytical solutions of the nonlinear initial boundary value problem in Michaelis-Menten kinetics have been derived. The modified Adomian decomposition method (MADM) is used to obtain the solutions for the non-linear model of an immobilized biocatalyst enzyme. Approximate analytical expressions for the concentration of substrate and the effective factor in immobilized biocatalyst enzymes are derived. The analytical solutions agree with the experimental results and numerical solutions (Matlab program) with and without external mass resistance for a slab, cylindrical and spherical pellets. These

analytical results are more descriptive and easy to visualize and optimize the kinetic parameters of immobilized enzymes.

Appendix A: Basic Concept of Modified Adomian Decomposition Method

Consider the singular boundary value problem of $n+1$ order nonlinear differential equation in the form

$$\begin{aligned} &y^{(n+1)}+\frac{m}{x}y^{(n)}+N\,y=g(x),\\ &y(0)=a_0,\ y'(0)=a_1,\ldots,y^{n-1}(0)=a_{n-1},\ y(b)=c \end{aligned} \tag{A.1}$$

Where N is a non-linear differential operator of order less than n , $g(x)$ is given, function and $a_0,a_1,\ldots a_{n-1},c,b$ are given constants. We propose the new differential operator, as below

$$L=x^{-1}\frac{d^n}{dx^n}x^{1+n-m}\frac{d}{dx}x^{m-n}(.) \tag{A.2}$$

Where $m\le n,\ n\ge 1$, so, the problem can be written as

$$L^{-1}(.)=g(x)-Ny \tag{A.3}$$

The inverse operator L^{-1} is therefore considered a $n+1$ fold integral operator, as below

$$L^{-1}(.)=x^{n-m}\int_b^x x^{m-n-1}\int_0^x\int_0^x\ldots\int_0^x x(.)\,dx\ldots dx. \tag{A.4}$$

By applying L^{-1} on (A.3), we have

$$y(x)=\varphi(x)+L^{-1}\,g(x)\,L^{-1}\,Ny \tag{A.5}$$

Such that $L\,\varphi(x)=0$

The Adomian decomposition method introduces the solution $y(x)$ and the nonlinear function Ny by infinite series

$$y(x)=\sum_{n=0}^{\infty}y_n(x) \tag{A.6}$$

and

$$Ny=\sum_{n=0}^{\infty}A_n \tag{A.7}$$

where the components $y_n(x)$ of the solution $y(x)$ will be determined recurrently. Specific algorithms were seen in [8, 12] to formulate Adomian polynomials. The following algorithm:

$$A_0=F(u),$$

$$A_1=F(u_0)u_1,$$

$$A_2=F(u_0)u_2+\frac{1}{2}F''(u_0)u_1^2,$$

$$A_2=F(u_0)u_2+\frac{1}{2}F''(u_0)u_1^2,$$

$$A_2=F(u_0)u_2+\frac{1}{2}F''(u_0)u_1^2,$$

$$A_3=F(u_0)u_3+\frac{1}{2}F''(u_0)u_1u_2+,\frac{1}{3!}F'''(u_0)u_1^3, \tag{A.8}$$

can be used constant Adomian polynomials, when $F(u)$ is a nonlinear function. By substituting (A. 6) and (A. 7) into (A. 5)

$$\sum_{n=0}^{\infty}y_n=\varphi(x)+L^{-1}g(x)-L^{-1}\sum_{n=0}^{\infty}A_n \tag{A.9}$$

Through using the modified Adomian decomposition method, the components $y_n(x)$ can be determined as

$$\begin{aligned} &y_0(x)=A+L^{-1}g(x)\\ &y_{n+1}(x)=-L^{-1}(A_n),\ n\ge 0 \end{aligned} \tag{A.10}$$

which gives

$$\begin{aligned} &y_0(x)=A+L^{-1}g(x)\\ &y_1(x)=-L^{-1}(A_0)\\ &y_2(x)=-L^{-1}(A_1)\\ &y_3(x)=-L^{-1}(A_2)\\ &\ldots \end{aligned} \tag{A.11}$$

From (A.8) and (A.11), we can determine the components $y_n(x)$, and hence the series solution of $y(x)$ in (A.6) can be immediately obtained. For numerical purposes, the n- term approximate

$$\psi_n=\sum_{n=0}^{n-1}y_k \tag{A.12}$$

can be used to approximate, the exact solution. The approach presented above can be validated by testing it on a variety of several linear and nonlinear initial value problems.

Appendix B: Analytical Solution of Substrate Concentration Without External Mass Transfer Resistance

The solutions of Eq. (1) for $g=3$ allow us to predict the concentration profiles of dimensionless substrate concentration in immobilized enzymes. In order to solve Eq.

(1), using the modified Adomian decomposition method, Eq. (1) can be written with the operator form

$$Ls = \left(\frac{\phi^2 C_0}{1+\beta_b C_0} \right) \tag{B.1}$$

where $L = \frac{d^2}{dx^2}$, Applying the inverse operator L^{-1} on both sides of Eq. (B. 1) yields

$$C(x) = Ax + B + \left(\frac{\phi^2 C_0}{1+\beta_b C_0} \right) \tag{B.2}$$

Where A and B are the constants of integration. We let,

$$C(x) = \sum_{n=0}^{\infty} C_n \tag{B.3}$$

$$N\left[C(x)\right] = \sum_{n=0}^{\infty} A_n \tag{B.4}$$

Where

$$N\left[C(x)\right] = \left(\frac{\phi^2 C_0}{1+\beta_b C_0} \right) \tag{B.5}$$

From the eqns (B. 3), (B. 4) and (B. 5), Eq. (B. 2) gives

$$\sum_{n=0}^{\infty} C_n(x) = Ax + B + \left(\frac{\phi^2 C_0}{1+\beta_b C_0} \right) \tag{B.6}$$

We identify the zeroth component as

$$C_0(x) = AX + B \tag{B.7}$$

And the remaining components as the recurrence relation

$$C_{n+1} = \phi^2 L^{-1} A_n ; n \geq 0 \tag{B.8}$$

where A_n are the Adomian polynomials of $C_0, C_1, \ldots, C_n$. We can find the first few A_n as follows:

Apply the boundary conditions in (B. 1) we get,

$$C_0 = 1 \tag{B.9}$$

Again to find C_1

$$C_1 = L^{-1}\left(\frac{\phi^2 C_0}{1+\beta_b C_0} \right) \tag{B.10}$$

Using (B. 9) in (B. 10),

$$C_1 = L^{-1}\left(\frac{\phi^2}{1+\beta_b} \right) \tag{B.11}$$

Again using this formula to find C_1,

$$C_1 = X^{-1} \int_0^X \int_0^X X\left(\frac{\phi^2}{1+\beta_b} \right) dXdX \tag{B.12}$$

Integrating Eqn. (B. 12),

$$C_1 = \left(\frac{\phi^2}{1+\beta_b} \right)\left(\frac{X^2}{6} + A + BX^{-1} \right) \tag{B.13}$$

Where A and B are integrating constants. Again using boundary conditions Eqn. (B. 13) becomes,

$$C_1 = \frac{\phi^2}{6(1+\beta_b)}\left(X^2 - 1\right) \tag{B.14}$$

Now, consider

$$C_2 = L^{-1}\left(\frac{1}{1!}\frac{d}{d\lambda} N\left(C_0 + C_1\lambda\right) \right)_{\lambda=0} \tag{B.15}$$

Solving $\left(\frac{1}{1!}\frac{d}{d\lambda} N\left(C_0 + C_1\lambda\right) \right)_{\lambda=0}$ we get,

$$C_2 = L^{-1}\left(\frac{\phi^4}{6(1+\beta_b)^3}\left(X^2 - 1\right) \right) \tag{B.16}$$

Therefore,

$$C_2 = X^{-1} \iint X\left(\frac{\phi^4}{6(1+\beta_b)^3}\left(X^2 - 1\right) \right) dXdX \tag{B.17}$$

Integrating Eqn. (B. 17),

$$C_2 = \left(\frac{\phi^4}{(1+\beta_b)^3} \right)\left(\frac{X^4}{120} - \frac{X^3}{36} + C + DX^{-1} \right) \tag{B.18}$$

Where C and D are integrating constants. Apply boundary conditions we get the value for C and D,

Therefore Eqn. (B. 17) in the form,

$$C_2 = \frac{\phi^4}{360\,(1+\beta_b)^3}\left(3X^4 - 10\,X^2 + 7\right) \tag{B.19}$$

Adding the Eqns. (B. 9), (B. 14) and (B. 19) we get the solution Eqn. (7). Similarly, to apply the above method for $g = 1$, $g = 2$ to find the solution.

Appendix C: Analytical Solution of Substrate Concentration with External Mass Transfer Resistance

The solutions of Eq. (1) for $g = 3$ allow us to predict the concentration profiles of dimensionless substrate concentration in immobilized enzymes. In order to solve Eq.

(1), using the modified Adomian decomposition method, Eq. (1) can be written with the operator form

$$Ls = \left(\frac{\phi^2 C_0}{1+\beta_b C_0} \right) \tag{C.1}$$

Where $L = \frac{d^2}{dx^2}$, Applying the inverse operator L^{-1} on both sides of Eq. (C.1) yields

$$C(x) = Ax + B + \left(\frac{\phi^2 C_0}{1+\beta_b C_0} \right) \tag{C.2}$$

Where A and B are the constants of integration. We let,

$$C(x) = \sum_{n=0}^{\infty} C_n \tag{C.3}$$

$$N\left[C(x)\right] = \sum_{n=0}^{\infty} A_n \tag{C.4}$$

Where

$$N\left[C(x)\right] = \left(\frac{\phi^2 C_0}{1+\beta_b C_0} \right) \tag{C.5}$$

From the eqns (C.3), (C.4) and (C.5), Eq. (C.2) gives

$$\sum_{n=0}^{\infty} C_n(x) = Ax + B + \left(\frac{\phi^2 C_0}{1+\beta_b C_0} \right) \tag{C.6}$$

We identify the zeroth component as

$$C_0(x) = AX + B \tag{C.7}$$

And the remaining components as the recurrence relation

$$C_{n+1} = \phi^2 L^{-1} A_n ; n \geq 0 \tag{C.8}$$

where A_n are the Adomian polynomials of $C_0, C_1, \ldots, C_n$. We can find the first few A_n as follows:

$$C = AX + B \tag{C.9}$$

Apply the boundary conditions in (C. 9) we get,

$$C_0 = 1 \tag{C.10}$$

Again to find C_1

$$C_1 = L^{-1}\left(\frac{\phi^2 C_0}{1+\beta_b C_0} \right) \tag{C.11}$$

Using (C. 10) in (C. 11),

$$C_1 = L^{-1}\left(\frac{\phi^2}{1+\beta_b} \right) \tag{C.12}$$

Again using this formula to find C_1,

$$C_1 = X^{-1} \int_0^X \int_0^X X \left(\frac{\phi^2}{1+\beta_b} \right) dXdX \tag{C.13}$$

Integrating Eqn. (C. 13),

$$C_1 = \left(\frac{\phi^2}{1+\beta_b} \right) \left(\frac{X^2}{6} + A + BX^{-1} \right) \tag{C.14}$$

Where A and B are integrating constants. Again, using boundary conditions Eqn. (C. 14) becomes,

$$C_1 = \frac{\phi^2}{1+\beta_b} \left(\frac{X^2}{6} - \frac{1}{3Bi} - \frac{1}{6} \right) \tag{C. 15}$$

Now, consider

$$C_2 = L^{-1}\left(\frac{1}{1!}\frac{d}{d\lambda} N\left(C_0 + C_1\lambda\right) \right)_{\lambda=0} \tag{C.16}$$

Solving $\left(\frac{1}{1!}\frac{d}{d\lambda} N\left(C_0 + C_1\lambda\right) \right)_{\lambda=0}$ we get,

$$C_2 = L^{-1}\left(\frac{\phi^4}{\left(1+\beta_b\right)^3} \left(\frac{X^2}{6} - \frac{1}{3Bi} - \frac{1}{6} \right) \right) \tag{C.17}$$

Therefore,

$$C_2 = X^{-1} \iint \left(\frac{\phi^4}{\left(1+\beta_b\right)^3} X \left(\frac{X^2}{6} - \frac{1}{3Bi} - \frac{1}{6} \right) \right) dXdX \tag{C.18}$$

Integrating Eqn. (C. 18),

$$C_2 = \left(\frac{\phi^4}{\left(1+\beta_b\right)^3} \right) \left(\frac{X^4}{120} - \frac{X^2}{6}\left(\frac{1}{3Bi} + \frac{1}{6} \right) + C + DX^{-1} \right) \tag{C.19}$$

Where C and D are integrating constants. Apply boundary conditions we get the value for C and D,

Therefore Eqn. (C. 11) in the form,

$$C_2 = \left(\frac{\phi^4}{\left(1+\beta_b\right)^3} \right) \left(\frac{1}{120}(X^4 - 1) - \left(\frac{1}{3Bi} + \frac{1}{6} \right) \left(\frac{X^2}{6} - \frac{1}{6} - \frac{1}{3Bi} \right) - \frac{1}{30Bi} \right) \tag{C.20}$$

Adding the Eqns. (C. 10), (C. 15) and (C. 20) we get the solution Eqn. (13). Similarly, to apply the above method for $g = 1$, $g = 2$ to find the solutions.

Appendix D1: Scilab Program for the Numerical Solution of Equation (11)

```
function pdex4
m = 0;
x=linspace(0, 1);
t = linspace(0, 10000000);
sol = pdepe(m, @pdex4pde, @pdex4ic, @pdex4bc, x, t);
u1 = sol(:, :, 1);
%————————————————————————————
figure
plot(x, u1(end, :))
title('u1(x, t)')
xlabel('Distance x')
ylabel('u1(x, 1)')
function [c, f, s] = pdex4pde(x, t, u, DuDx);
c=1;
f =1.* DuDx;
a=6; b=5;
F =-((a^2*u(1))/((1+b*u(1))));
s =F;
% ————————————————————————————
function u0 = pdex4ic(x);
u0 = [0];
% ————————————————————————————
function [pl, ql, pr, qr] = pdex4bc(xl, ul, xr, ur, t)
pl = [0];
ql = [1];
pr = [ur(1)-1];
qr = [0];
```

Appendix D2: Scilab Program for the Numerical Solution of Equation (13)

```
function pdex4
m = 0;
x = linspace(0, 1);
t = linspace(0, 1000000);
sol = pdepe(m, @pdex4pde, @pdex4ic, @pdex4bc, x, t);
u1 = sol(:, :, 1);
% ————————————————————————————
figure
plot(x, u1(end,:))
title('u1(x, t)')
xlabel('Distance x')
ylabel('u1(x, 1)')
function [c, f, s] = pdex4pde(x, t, u, DuDx)
c =1;
f =1.* DuDx;
e=1; alpha=5;
F =-(e*u(1))/((1+(alpha*u(1))));
s =F;
% ————————————————————————————
function u0 = pdex4ic(x)
u0 = [0];
% ————————————————————————————
function [pl, ql, pr, qr] = pdex4bc(xl, ul, xr, ur, t)
B=1;
pl = [0];
ql = [1];
pr = [-B*(1-ur(1))];
qr = [1];
```

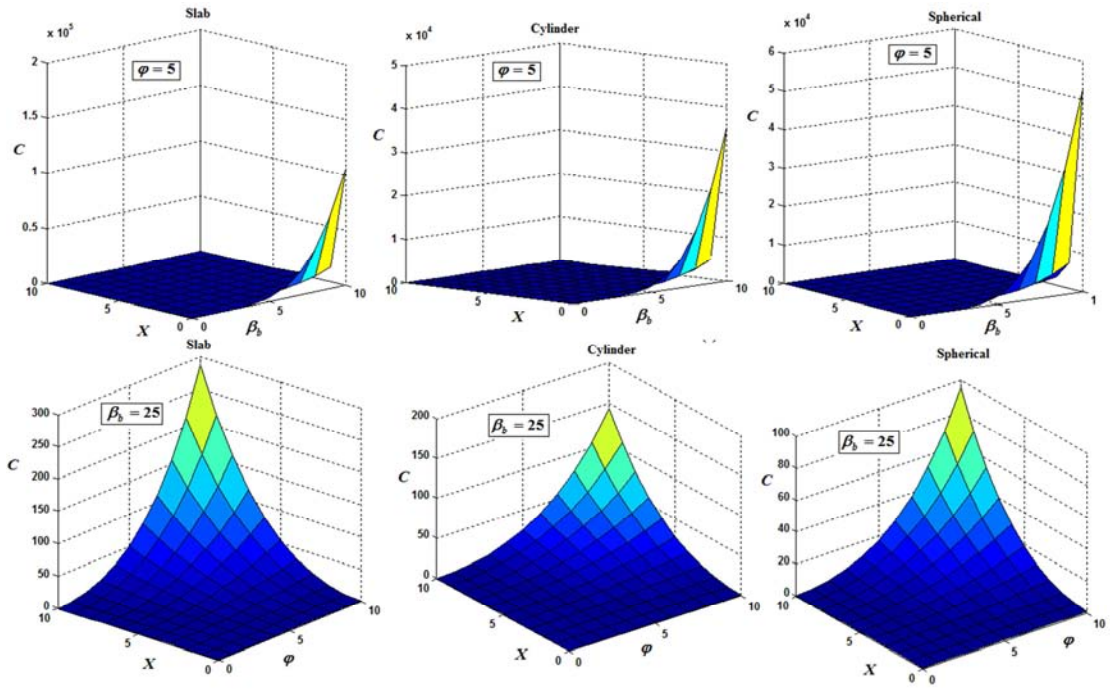

(i). Michaelis-Menten constant β_b, (ii). Thiele modulus ϕ.

Figure 12. *Plot of the three-dimensional dimensionless concentration C against the dimensionless distance X for the three pellets calculated using Eqn. (11) (without mass-transfer resistance).*

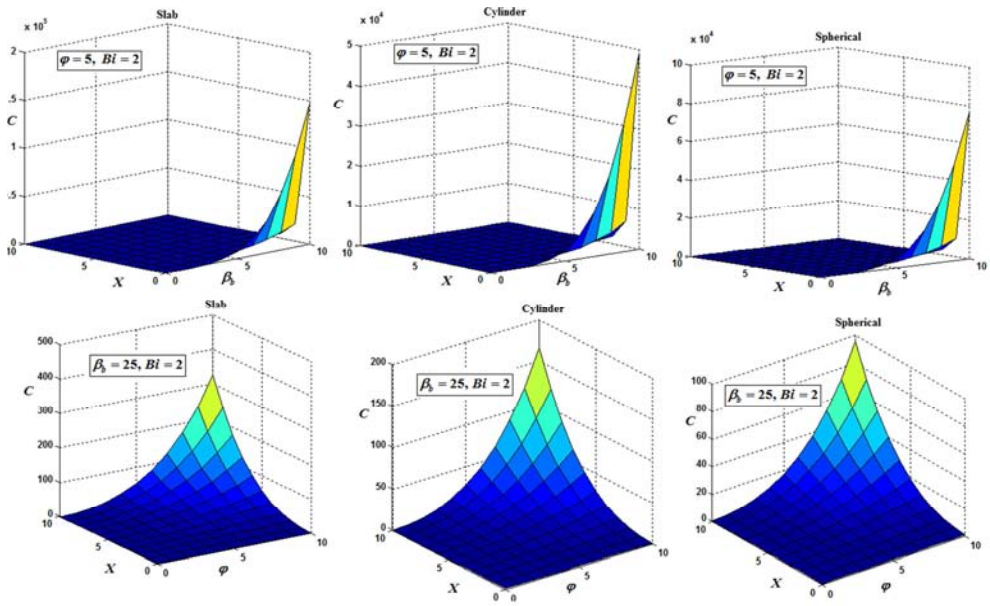

(i). Michaelis-Menten constant β_b , (ii). Thiele modulus ϕ

Figure 13. *Plot of the three-dimensional dimensionless concentration C against the dimensionless distance X for the three pellets calculated using Eqn. (14) (with mass-transfer resistance).*

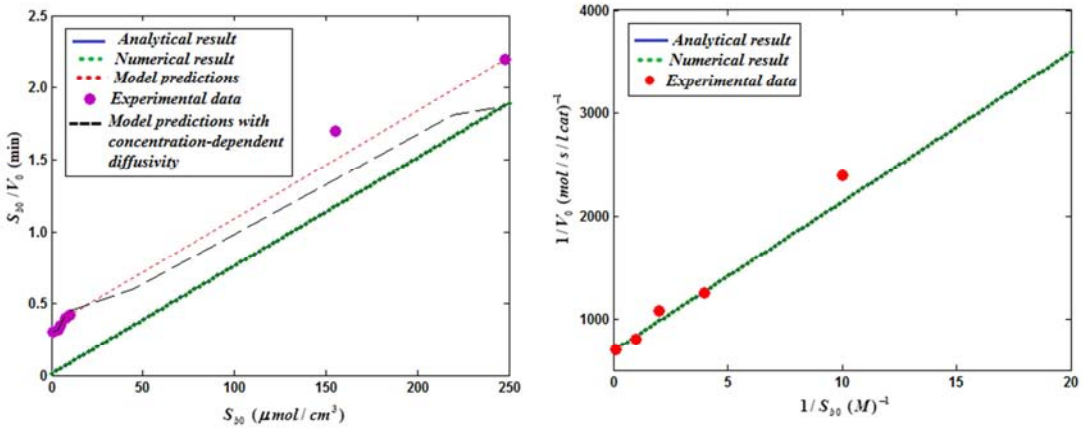

Figure 14. *Hanes-Woolf plot for case 2 in the absence of mass transfer limitations (dotted line), model predictions with constant diffusivity (dot-dashed line), model predictions with concentration-dependent diffusivity (dashed line), experimental data (symbols), and analytical result (solid line).*

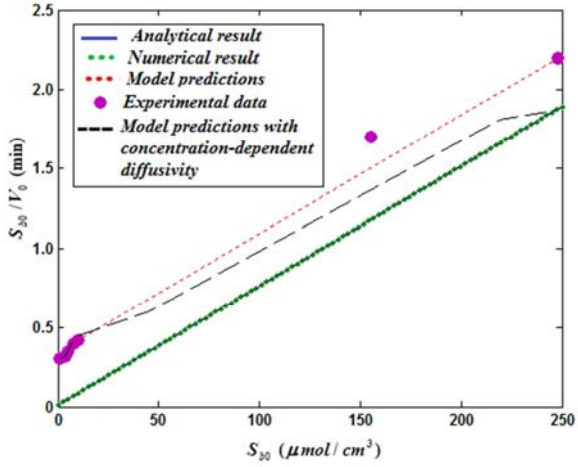

Figure 15. *Line weaver-Burk plot for case 2; model predictions using the optimized parameters (dotted line), experimental data (symbols) and analytical result (solid line).*

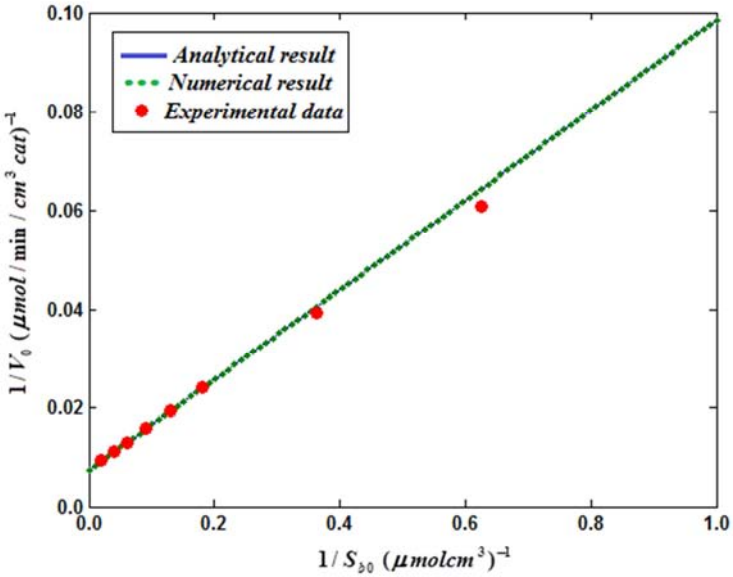

Figure 16. *Line weaver-Burk plot for the forward reaction of case 3; model predictions using the optimized parameters (dotted line), experimental data (symbols) and analytical result (solid line).*

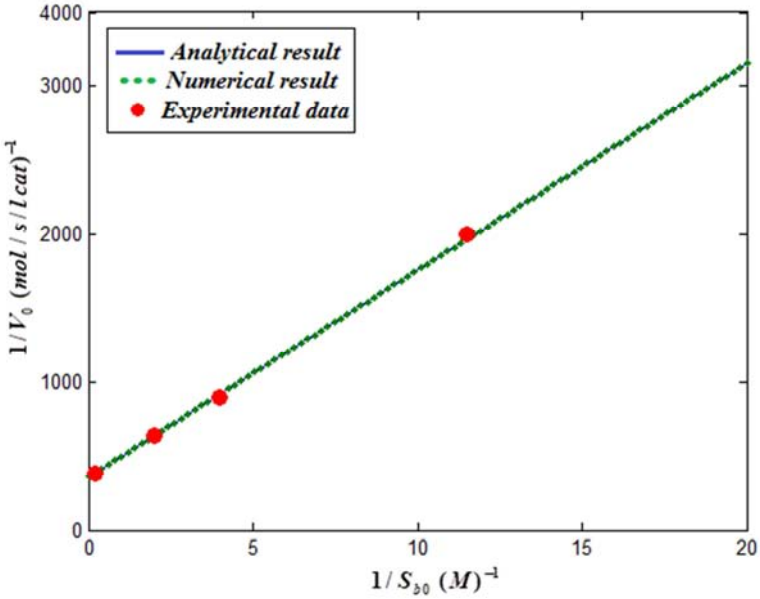

Figure 17. *Line weaver-Burk plot for the forward reaction of case 4; model predictions using the optimized parameters (dotted line), experimental data (symbols) and analytical result (solid line).*

References

[1] R. Aris, The Mathematical Theory Of Diffusion And Reaction In Permeable Catalysts, Clarendon, Oxford. 1975.

[2] P. Cheviollotte, Relation between the reaction cytochrome oxidase-Oxygen and oxygen uptake in cells in vivo-The role of diffusion, J. Theoret. Biol. 39: 277-295, (1973).

[3] M. Moo-Young and T. Kobayashi, Effectiveness factors for immobilized-enzyme reactions, Can&. J. Chem. Eng. 50: 162-167 (1972).

[4] S. A. Mireshghi, A. Kheirolomoom and F. khorasheh, Application of an optimization algotithem for estimation of substrate mass transfer parameters for immobilized enzyme reactions, Scientia Iranica, 8(2001)189-196.

[5] Benaiges, M. D., Sola, C., and de Mas, C.: Intrinsic kinetic constants of an immobilized glucose isomerase. J. Chem. Technol. Biotechnol., 36, 480-486 (1986).

[6] Shiraishi, F. 'Substrate concentration dependence of the apparent maximum reaction rate and Michaelis-Menten constant in immobilized enzyme reactions'. Int. Chem. Eng., 32, 140-147 (1992).

[7] Shiraishi, F., Hasegawa, T., Kasai, S., Makishita, N., and Miyakawa, H.: Characteristics of apparent kinetic parameters in a packed bed immobilized enzyme reactor. Chem. Eng. Sci., 51, 2847-2852 (1996).

[8] Lortie, R. and Andre, G.: On the use of apparent kinetic parameters for enzyme bearing particles with internal mass transfer limitations. Chem. Eng. Sci., 45, 1133-l 136 (1990).

[9] Hemrik Pedersen, EnmoAdema, K. Venkatasubramanian, P. V. Sundaram, 'Estimation of intrinsic kinetic parameters in tubular enzyme reactors by a direct approach', Applied Biochemistry and Biotechnology, 1985, Volume 11, Issue 1, pp 29-44.

[10] V. Bales and P. Rajniak, 'Mathematical simulation of fixed bed reactor using immobilized enzymes', Chemical Papers, 40 (3), 329–338 (1986).

[11] Messing, R. A., Immobilized Enzyme for Industrial Reactors, Academic Press, New York (1975).

[12] Wilhelm Tischer, Frank Wedekind, 'Immobilized Enzymes: Methods and Applications', Topics in Current Chemistry, Vol. 200© Springer Verlag Berlin Heidelberg 1999.

[13] Engasser, J. M. and Horvath, C.: Diffusion and kinetics with immobilized enzymes, p. 127-220.

[14] Farhadkhorasheh, Azadehkheirolomoom, and Seyedalirezamireshghi, 'application of an optimization algorithm for estimating intrinsic kinetic parameters of immobilized enzymes', journal of bioscience and bioengineering, vol. 94, no. 1, l-7. 2002.

[15] Houng, J. Y., Yu, H., Chen, K. C., and Tiu, C.: Analysis ofsubstrate protection of an immobilized glucose isomerasereactor. Biotechnol. Bioeng., 41, 451458 (1993).

[16] G. Adomian, Convergent series solution of nonlinear equations, J. Comp. App. Math. 11(1984) 225-230.

[17] N. A. Hassan Ismail et al, Comparison study between restrictive Taylor, restrictive Pade´approximations and Adomian decomposition method for the solitary wave solution of the General KdV equation, Appl. Math. Comp. 167 (2005) 849–869.

[18] A. M. Wazwaz, A reliable modification of ADM, Appl. Math. Comp. 102 (1) (1999) 77-86.

[19] Yahya Q. H., Liu M. Z., "Solving singular boundary value problems of higher-order ordinary differential equations by modified Adomian decomposition method", Commun. Nonlinear Sci. Numer. Simulat, doi: 10.1016/j.cnsns.2008.09.02 14 (2009) 2592–2596.

[20] Yahya Q. H., "Modified Adomian decomposition method for second order singular initial value problems", Advances in computational mathematics and its applications, vol. 1, No. 2, 2012.

[21] B. Muatjetjeja, C. M. Khalique, Exact solutions of the generalized Lane–Emden equations of the first and second kind. Pramana 77, 545–554 (2011).

[22] J.-S. Duan. R. Rach, A. M. Wazwaz, Steady-state concentrations of carbon dioxide absorbed into phenyl glycidyl ether solutions by the Adomian decomposition method. J. Math. Chem., 53, 1054–1067 (2015).

[23] R. Rach, J. S. Duan, A. M. Wazwaz, On the solution of non-isothermal reaction–diffusion model equations in a spherical catalyst by the modified Adomian method, Chem. Eng. Comm., 202(8), 1081–1088 (2015).

[24] A. Saadatmandi, N. Nafar, S. P. Toufighi, Numerical study on the reaction– diffusion process in a spherical biocatalyst. Iran. J. Mathl. Chem., 5, 47–61 (2014).

[25] V. Ananthaswamy, L. Rajendran, Approximate Analytical Solution of Non-Linear Kinetic Equation in a Porous Pellet, Global Journal of Pure and Applied Mathematics Volume 8, Number 2 (2012), pp. 101-111.

[26] S. Sevukaperumal, L. Rajendran, Analytical solution of the Concentration of species using modified adomian decomposition method, International Journal of mathematical Archive-4(6), 2013, 107-117.

[27] T. Praveen, Pedro Valencia, L. Rajendran, Theoretical analysis of intrinsic Reaction kinetics and the behavior of immobilized Enzymes system for steady-state conditions, Biochemical Engineering Journal, 91, 2014, pp. 129-139.

[28] V. Meena, T. Praveen, and L. Rajendran, mathematical Modeling and analysis of the Molar Concentrations of Ethanol, Acetaldehyde and Ethyl Acetate Inside the Catalyst Particle. ISSN 00231584, Kinetics and Catalysis, 2016, Vol. 57, No. 1, pp. 125–134.

[29] S. Liao, J. Sub, A. T. Chwang, Series solutions for a nonlinear model of combined convective and radiative cooling of a spherical body, Int. J. Heat Mass Tran., 49, 2437–2445 (2006).

[30] V. Ananthaswamy, R. Shanthakumari, M. Subha, Simple analytical expressions of the non–linear reaction diffusion process in an immobilized biocatalyst particle using the new homotopy perturbation method, Review of Bioinformatics and Biometrics. 3, 23– 28 (2014).

[31] J.-H. He, "Application of homotopy perturbation method to nonlinear wave equations," Chaos, Solitons and Fractals, vol. 26, no. 3, pp. 695–700, 2005.

[32] Q. K. Ghori, M. Ahmed, and A. M. Siddiqui, "ApplicationofHomotopy perturbation method to squeezing flow of anewtonian fluid," International Journal of Nonlinear Sciencesand Numerical Simulation, vol. 8, no. 2, pp. 179–184, 2007.

[33] S.-J. Li and Y.-X. Liu, "An improved approach to nonlineardynamical system identification using PID neural networks,"International Journal of Nonlinear Sciences and Numerical Simulation, vol. 7, no. 2, pp. 177–182, 2006.

[34] L. Rajendran and S. Anitha, "Reply to 'Comments on analyticalsolution of amperometric enzymatic reactions based onHPM', ElectrochimicaActa, vol. 102, pp. 474–476, 2013.

[35] MATLAB 6. 1, The Math Works Inc., Natick, MA (2000), www.scilabenterprises.com.